Death Protein 5 and p53-Upregulated Modulator of Apoptosis Mediate the Endoplasmic Reticulum Stress–Mitochondrial Dialog Triggering Lipotoxic Rodent and Human β-Cell Apoptosis

Daniel A. Cunha,[1] Mariana Igoillo-Esteve,[1] Esteban N. Gurzov,[1] Carla M. Germano,[1] Najib Naamane,[1] Ihsane Marhfour,[1] Makiko Fukaya,[1] Jean-Marie Vanderwinden,[2] Conny Gysemans,[3] Chantal Mathieu,[3] Lorella Marselli,[4] Piero Marchetti,[4] Heather P. Harding,[5] David Ron,[5] Décio L. Eizirik,[1] and Miriam Cnop[1,6]

Environmental factors such as diets rich in saturated fats contribute to dysfunction and death of pancreatic β-cells in diabetes. Endoplasmic reticulum (ER) stress is elicited in β-cells by saturated fatty acids. Here we show that palmitate-induced β-cell apoptosis is mediated by the intrinsic mitochondrial pathway. By microarray analysis, we identified a palmitate-triggered ER stress gene expression signature and the induction of the BH3-only proteins death protein 5 (DP5) and p53-upregulated modulator of apoptosis (PUMA). Knockdown of either protein reduced cytochrome *c* release, caspase-3 activation, and apoptosis in rat and human β-cells. *DP5* induction depends on inositol-requiring enzyme 1 (IRE1)–dependent c-Jun NH_2-terminal kinase and PKR–like ER kinase (PERK)–induced activating transcription factor (ATF3) binding to its promoter. *PUMA* expression is also PERK/ATF3-dependent, through tribbles 3 (TRB3)–regulated AKT inhibition and FoxO3a activation. $DP5^{-/-}$ mice are protected from high fat diet–induced loss of glucose tolerance and have twofold greater pancreatic β-cell mass. This study elucidates the crosstalk between lipotoxic ER stress and the mitochondrial pathway of apoptosis that causes β-cell death in diabetes. ***Diabetes*** **61:2763–2775, 2012**

The global prevalence of type 2 diabetes (T2D) has reached 250 million and is projected to increase to nearly 400 million by 2030 (1). The consumption of a hypercaloric diet rich in saturated fats, in the setting of an unfavorable genetic background, is causal in the pathogenesis of T2D. Insulin resistance in peripheral tissues is a prime feature of T2D, but diabetes only develops in patients who are unable to sustain a compensatory increase in insulin release by the pancreatic β-cells. The loss of β-cell mass by apoptosis contributes to the progressive β-cell failure in T2D (2). Dietary or adipocyte-derived free fatty acids (FFAs) contribute both to peripheral insulin resistance and to β-cell dysfunction and death in T2D. Chronic high-fat diet (HFD) leads to hyperglycemia as a consequence of impaired insulin secretion and insulin resistance (3,4), and in vitro exposure to saturated and, to a lesser extent, unsaturated FFAs induces β-cell dysfunction and death (5,6).

How FFAs cause β-cell apoptosis is not well understood. Several studies have indicated endoplasmic reticulum (ER) stress as a potential mediator (7–10). Perturbations in ER function initiate the unfolded protein response (UPR) governed by three ER transmembrane proteins: PKR–like ER kinase (PERK), inositol-requiring kinase-1 (IRE1), and activating transcription factor (ATF) 6. The prime function of the UPR is to restore ER homeostasis by reducing protein load and increasing ER folding capacity and misfolded protein degradation. Attenuation of protein translation is executed by PERK through phosphorylation of the eukaryotic translation initiation factor 2α (eIF2α), whereas the two other branches increase ER function by upregulating ER chaperones and the ER-associated protein degradation machinery. Nonresolved ER stress induces cell death (11,12). ER stress may contribute to β-cell failure in T2D, because increased expression of markers of ER stress, including ATF3 and C/EBP homologous protein (CHOP; also known as GADD153 or DDIT3), has been found in islets from T2D patients (11). Prolonged eIF2α phosphorylation induces β-cell apoptosis through the mitochondrial pathway of cell death (13–15), but how lipotoxic ER stress response culminates in the triggering and execution of β-cell apoptosis remains unknown.

The intrinsic or mitochondrial pathway of cell death is tightly modulated by proteins of the B-cell lymphoma (Bcl) 2 family, composed of antiapoptotic (Bcl-2, Bcl-XL, Bcl-w, myeloid cell leukemia sequence [Mcl] 1, and A1) and proapoptotic members that are further subdivided in multidomain (Bax, Bak, and Bok) and BH3-only proteins (death protein 5 [DP5, also known as harakiri], Bim, Bid, p53-upregulated modulator of apoptosis [PUMA, also known as BBC3], Bad, and Noxa) (16). Apoptosis starts with Bax translocation from the cytosol to the mitochondrial membrane, where it oligomerizes with Bak. The pore formed by Bax/Bak causes mitochondrial outer membrane permeabilization, allowing soluble proteins such as cytochrome *c* to

From the [1]Laboratory of Experimental Medicine, Université Libre de Bruxelles, Brussels, Belgium; the [2]Laboratory of Neurophysiology, Université Libre de Bruxelles, Brussels, Belgium; the [3]Laboratory of Experimental Medicine Endocrinology (LEGENDO), Faculty of Medicine, Katholieke Universiteit Leuven, Leuven, Belgium; the [4]Department of Endocrinology and Metabolism, University of Pisa, Pisa, Italy; the [5]University of Cambridge Metabolic Research Laboratories and NIHR Cambridge Biomedical Research Centre, Cambridge, U.K.; and the [6]Division of Endocrinology, Erasmus Hospital, Université Libre de Bruxelles, Brussels, Belgium.
Corresponding author: Miriam Cnop, mcnop@ulb.ac.be.
Received 7 February 2012 and accepted 4 May 2012.
DOI: 10.2337/db12-0123
This article contains Supplementary Data online at http://diabetes.diabetesjournals.org/lookup/suppl/doi:10.2337/db12-0123/-/DC1.
E.N.G. is currently affiliated with the Department of Biochemistry and Molecular Biology, School of Biomedical Sciences, Monash University, Melbourne, Australia.

diffuse to the cytosol. The subsequent formation of the apoptosome leads to caspase 9 activation and caspase 3–mediated cell death. The BH3-only proteins induce apoptosis in a cell type- and stimulus-dependent fashion. These proteins are essential initiators of apoptosis by their ability to bind and inhibit prosurvival Bcl-2 members and by their direct activation of Bax and Bak (17). The BH3-only proteins are transcriptionally regulated, and some, including Bim and Bid, are posttranslationally modified. The c-Jun NH_2-terminal kinase (JNK) plays an important role in the regulation of the mitochondrial pathway of apoptosis (18). JNK activates Bax, Bim, and Bad by phosphorylation (19–21) and upregulates Bim, PUMA, and DP5 in hepatocytes and neurons (22,23).

In this study, we have used global gene expression analyses followed by a comprehensive series of focused experiments to characterize the pathways of apoptosis in lipotoxic β-cell death and their regulation by the ER stress response. We demonstrate that the activation of JNK and PERK by palmitate contributes to induction of the BH3-only proteins DP5 and PUMA, and we clarify the ER stress–mitochondrial dialog triggering lipotoxic β-cell apoptosis, thus suggesting novel targets for the prevention of β-cell demise in early T2D.

RESEARCH DESIGN AND METHODS

Culture of INS-1E and primary fluorescence activated cell sorter–purified rat β- and human islet cells and functional studies. The culture of INS-1E and primary fluorescence activated cell sorter–purified rat β-cells is described in the Supplementary Data.

Human islets (from 4 donors aged 63 ± 7 years, BMI 25 ± 1 kg/m^2, cause of death cerebral hemorrhage) were isolated by collagenase digestion and density gradient purification. The islets were cultured, dispersed, and transfected as described previously (24). The percentage of β-cells, examined by insulin immunofluorescence (9), was 69 ± 11%.

For FFA exposure, primary β-cells were cultured in medium with 1% BSA without FBS, and INS-1E cells were cultured in medium with 1% FBS and 1% BSA (5). Oleate and palmitate (Sigma, Schnelldorf, Germany) were dissolved in 90% ethanol (6) and used at a final concentration of 0.5 mmol/L, which in the presence of 1% BSA results in unbound FFA concentrations in the nanomolar range (5). The chemical JNK inhibitor SP600125 (Sigma) and the peptide JNK inhibitor L-TAT-JNKi were used at 10 μmol/L for 2 h before and during FFA exposure (9). The IRE1 inhibitor 4μ8C was used at 25 μmol/L during FFA exposure (25).

Details on the microarray analysis, real-time PCR primers, RNA interference, chromatin immunoprecipitation (ChIP), promoter reporter assay, and antibodies are provided in the Supplementary Data.

Assessment of β-cell apoptosis. Apoptotic β-cells and INS-1E cells were counted in fluorescence microscopy after staining with the DNA-binding dyes propidium iodide (5 μg/mL) and Hoechst 33342 (10 μg/mL) (15). Apoptosis was confirmed by additional methods, including Bax translocation, caspase 9 and 3 cleavage, and cytochrome *c* release, measured as described elsewhere (13).

Mouse studies. Male *DP5*$^{-/-}$ and wild type (WT) C57BL/6 J mice were given standard chow (fat 10% of caloric intake, D12450B) or HFD (fat 60% of caloric intake, D12492; Research Diets). After 12 weeks, intraperitoneal glucose tolerance tests were done in 16-h fasted mice by injecting glucose (2 mg/g body weight). Blood was collected from the tail at times 0, 15, 30, 60, 90, and 120 min, and glucose was measured with a FreeStyle Lite glucometer (Abbott Diabetes Care). Plasma was separated by centrifugation (10 min, 5000*g*) and stored at −20°C. Plasma insulin was measured with the Ultrasensitive Mouse ELISA Kit (Crystal Chem, Downers Grove, IL). For the intraperitoneal insulin tolerance test, 0.75 mU/g body weight Actrapid (Novo Nordisk) was injected after a 4-h fast, and glucose was measured at the time points listed previously.

β-Cell mass. Pancreases were taken from mice killed after 25 weeks on the different diets. Three nonconsecutive 5-μm thick pancreatic sections 150 μm apart were labeled with a standard immunoperoxidase method for paraffin sections with a mouse anti-insulin antibody (1/4000; Sigma). The β-cell mass was quantified blindly as β-cell volume density multiplied by pancreas weight (26). To assess β-cell size, nuclear crowding was determined as the number of β-cell nuclei per 100 μm^2 β-cell cytoplasm (27). The β-cell proliferation was examined as described in the Supplementary Data.

Glucose-stimulated insulin secretion. After isolation, *DP5*$^{-/-}$ and WT mouse islets were cultured for 30 min in M199 medium containing 5.6 mmol/L glucose and washed with modified Krebs-Ringer bicarbonate HEPES solution (150 mmol/L NaCl, 3.5 mmol/L KCl, 0.5 mmol/L $MgCl_2$, 1.5 mmol/L $CaCl_2$, 5 mmol/L $NaHCO_3$, 0.5 mmol/L NaH_2PO_4, 10 mmol/L HEPES, and 0.1% BSA at pH 7.4). Insulin secretion was induced by 1 h of incubation with Krebs-Ringer bicarbonate HEPES solution containing 1.7 or 16.7 mmol/L glucose. Insulin was measured by ELISA in cell-free supernatants and acid-ethanol extracted cell lysates.

Statistical analysis. Data are presented as means ± SE of the indicated number (n) of independent experiments. Comparisons were performed by ANOVA, followed by paired t test with the Bonferroni correction for multiple comparisons. $P < 0.05$ was considered statistically significant.

RESULTS

Palmitate induces β-cell death through the mitochondrial pathway of apoptosis. Palmitate induced cytochrome *c* release from the mitochondria (Fig. 1*A*–C), Bax translocation from the cytosol to the mitochondria (Fig. 1*B-D*), and caspase 9 and 3 activation (Fig. 1*E*), demonstrating that palmitate engages the intrinsic pathway of apoptosis in pancreatic β-cells. Oleate induces less cell death (5,13) and does not stimulate cytochrome *c* release. In a time-course study, palmitate decreased Bcl-2 protein expression from 16 h on, independently of *BCL2* mRNA expression (Supplementary Fig. 1). Knockdown of Bcl-2 induced apoptosis and sensitized cells to FFAs (Supplementary Fig. 1*B*). Palmitate also reduced Bcl-XL protein levels though at a late time-point of 24 h only (Supplementary Fig. 2*A*). Similar to Bcl-2, Bcl-XL knockdown induced β-cell apoptosis (Supplementary Fig. 2*B*). These results confirm the antiapoptotic role of Bcl-2 and Bcl-XL in β-cells under basal and lipotoxic conditions. The mitochondrial morphology of palmitate-treated cells was punctate, as opposed to the reticular adenosine 5′-triphosphate (ATP) synthase β staining in control cells (Supplementary Fig. 1*C* and *D*), and this coincided with the marked decrease in Bcl-2 protein expression, suggesting that Bcl-2 depletion by palmitate contributes to disruption of the mitochondrial network.

Palmitate modulates cell death and other gene networks in β-cells. We next profiled the global gene expression of INS-1E cells exposed to palmitate for 6 and 14 h. In the array analysis, 20,405 probe sets corresponding to 10,524 genes were detected as present in control or palmitate-treated β-cells. Palmitate modified the expression of 6.7% (792 genes) and 8.2% (1,074 genes) of probe sets at 6 and 14 h, respectively. The top functional clusters included gene expression, lipid metabolism, cell growth, cellular function and maintenance, and cellular compromise at 6 h and cell death, cellular function, cellular compromise, protein synthesis, and lipid metabolism at 14 h. Two networks were enriched in proapoptotic signaling molecules. At 6 h, palmitate upregulated markers of ER stress, including ATF4, ATF3, CHOP, growth arrest and DNA damage protein 34, and TRB3 (Supplementary Fig. 3), which is in keeping with our previous findings on the proapoptotic signaling in the PERK branch of the UPR (9,15). At 14 h, we detected a network of mitochondrial cell death genes containing *DP5* and *PUMA*, *PERK*, and *Jun* upregulations (Supplementary Fig. 4).

Genes were also classified by a previously described manual curation (28) according to their potential role in β-cell dysfunction and death (Supplementary Table 1). Palmitate decreased the expression of glucose metabolism genes involved in glycolysis and the citric acid cycle, and upregulated lipid metabolism genes such as *Acsl*, *Cpt1a*,

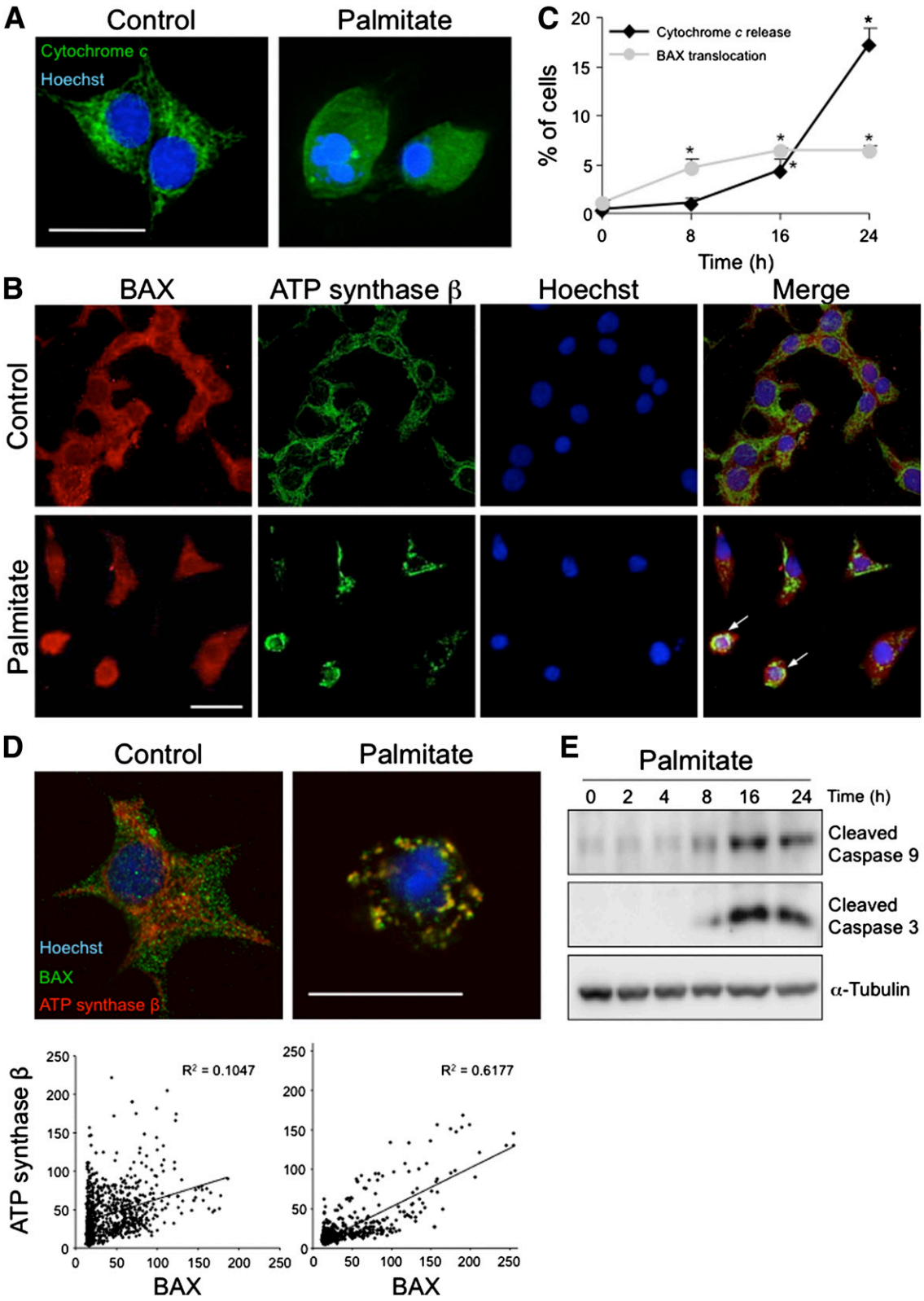

FIG. 1. Palmitate induces apoptosis through the mitochondrial pathway. *A*: Representative immunofluorescence images of INS-1E cells exposed to palmitate for 24 h and stained for cytochrome *c* (green) and DNA (with Hoechst 33342, blue) (bar 20 μm). *B*: Representative immunofluorescence pictures of INS-1E cells treated with palmitate for 24 h and stained for Bax (red), ATP synthase β (green), and DNA (Hoechst, blue) (bar represents 20 μm). Arrows point to cells with Bax translocation to the mitochondria. *C*: Percentage of INS-1E cells with mitochondrial Bax translocation or cytochrome *c* release after palmitate treatment for the indicated periods (n = 3–4). *D*: Confocal microscopy of INS-1E cells treated with palmitate for 24 h and stained for Bax (green), ATP synthase β (red), and DNA (Hoechst, blue) (*top*). Scatterplots of fluorescence intensities measured by line scanning in confocal microscopy images for Bax and ATP synthase β of 3 control and 4 palmitate-treated cells. Linear regression shows a tight correlation in palmitate-treated cells (*bottom right*) compared with control condition (*bottom left*), suggestive of Bax translocation to the mitochondria. *E*: Time course of caspase 9 and 3 activation analyzed by Western blot in palmitate-treated INS-1E cells. A representative blot of 3 independent experiments is shown. *$P < 0.05$ against control. (A high-quality digital representation of this figure is available in the online issue.)

and *Fads1*. The AP-1 family of transcription factors, including *c-Jun* and *c-Fos*, was induced at both time points. Genes mediating ER function and signal transduction in the different branches of the UPR were induced, including *ATF3*, *ATF4*, *CHOP*, and *TRB3* and also *Sec61a1* and *Dnajc3* (Supplementary Table 1). The mRNA expressions of prodeath genes such as *Bax*, *Bak*, and *Bim* were not significantly modified; however, the BH3-only proteins DP5 and PUMA were markedly upregulated. On the basis of these gene expression analyses, these two Bcl-2 members were further studied for their role in mitochondrial β-cell death.

The BH3-only proteins DP5 and PUMA contribute to palmitate-induced apoptosis. By real-time PCR, we confirmed the array finding that palmitate induced *DP5* expression, with a maximum after 16 h (Fig. 2*A*). On the other hand, oleate did not induced *DP5* expression (Fig. 2*A*). Efficient DP5 knockdown by RNA interference (Fig. 2*B*) reduced cytochrome *c* release, caspase 3 activation, and apoptosis in palmitate-treated cells (Fig. 2*C* and *D*) but did not prevent the mild oleate-induced apoptosis (Fig. 2*D*). Palmitate induced *DP5* in primary rat β-cells (Fig. 2*E*), and DP5 knockdown partially protected β-cells against palmitate (Fig. 2*E*). In human islet cells, palmitate also induced *DP5* (Fig. 2*F*), and DP5 knockdown protected cells from lipotoxicity (Fig. 2*F*).

PUMA was markedly induced by palmitate, peaking at 16 h, but not by oleate (Fig. 3*A*). Knockdown of PUMA (Fig. 3*B*) decreased palmitate-induced cytochrome *c* release, caspase 3 activation, and apoptosis (Fig. 3*C* and D), whereas it did not affect oleate toxicity (Fig. 3*D*). Palmitate also upregulated *PUMA* expression in fluorescence activated cell sorter–purified rat β-cells and human islet cells (Fig. 3*E* and F). *PUMA* RNA interference partially (Fig. 3*E*) and nearly completely (Fig. 3*F*) prevented palmitate toxicity in, respectively, primary rat β-cells and human islet cells. As a negative control, we studied a gene that was not detected as changed in the array analysis, namely *Bim*. Unlike DP5 and PUMA, *Bim* was not induced by palmitate (Supplementary Fig. 2*C*), and knockdown of its protein product did not modify apoptosis rates (Supplementary Fig. 2*D*), confirming that *Bim* does not play a major role in lipotoxic β-cell death.

JNK mediates the lipotoxic induction of *DP5* but not *PUMA*. To assess the mechanism by which palmitate induces *DP5* expression, a *DP5* promoter luciferase reporter was used. The promoter sequence between −125 to −85 is important for DP5 induction by palmitate, because its deletion reduced promoter activity by 42% compared with the full construct (Fig. 4*A*). This promoter region has a conserved ATF site where c-Jun binds after phosphorylation by JNK (23). Palmitate activated JNK and its target c-Jun from 30 min onward, peaking at 4–8 h (Supplementary Fig. 5*A* and *B*). JNK inhibition by SP600125 reduced c-Jun phosphorylation (Fig. 4*B*) and abrogated palmitate-induced *DP5* promoter activation and mRNA expression both in INS-1E cells (Fig. 4*C* and D) and in primary β-cells (Fig. 4*D*). The small peptide JNK inhibitor L-TAT-JNKi, previously shown to inhibit JNK and protect β-cells against palmitate treatment (9), produced a similar reduction of c-Jun phosphorylation and decreased palmitate-induced *DP5* expression (Supplementary Fig. 5*C* and *D*). The *p*-c-Jun binding to the *DP5* promoter was increased by palmitate as observed in ChIP experiments (Fig. 4*E*), suggesting that *p*-c-Jun transcriptionally induces *DP5*. IRE1α knockdown (by 76 ± 3%) reduced *XBP1* splicing (by 46 ± 6%) and decreased palmitate-induced JNK phosphorylation (Fig. 4*F*). Additional support for the role of IRE1 was provided by using the novel IRE1 inhibitor 4μ8C (25). This small molecule very effectively blocked IRE1, inhibiting spliced *XBP1* expression by 96 ± 1%, and significantly decreased JNK phosphorylation and *DP5* expression (Fig. 4*G* and *H*), confirming that IRE1-JNK mediates the *DP5* induction. 4μ8C did not inhibit JNK phosphorylation by interleukin-1β and interferon-γ, suggesting it does not directly inactivate JNK (data not shown).

PUMA expression is controlled by different transcription factors, including p53 and nuclear factor-κB (NF-κB) (29,30). Time course experiments showed that p53 is not induced by palmitate in INS-1E cells, suggesting a p53-independent PUMA regulation in β-cells (Supplementary Fig. 5*E*). The activation of the *PUMA* promoter by palmitate was not affected by mutation of the NF-κB binding site (Supplementary Fig. 5*F*), previously shown to be important for cytokine-mediated *PUMA* upregulation (31). Furthermore, *PUMA* promoter activity and *PUMA* mRNA induction were not modified by JNK inhibitors (Supplementary Fig. 5*G–I*), suggesting a different role for JNK in the regulation of the *DP5* and *PUMA* promoters.

PERK-ATF3 signaling induces *DP5* and *PUMA*. The PERK pathway and its downstream effectors CHOP and TRB3 are proapoptotic in palmitate-treated β-cells (9,15,32). Knockdown of PERK by small interfering RNA (siRNA) decreased basal and palmitate-induced eIF2α phosphorylation (Supplementary Fig. 6*A–C*) but did not prevent JNK activation (Supplementary Fig. 6*D*). PERK knockdown reduced *DP5* and *PUMA* inductions by palmitate (Fig. 5*A* and B). Knockdown of ATF4 or CHOP did not affect the induction of either BH3-only protein by palmitate (Supplementary Fig. 6*E–H*). ATF3 siRNA, however, mimicked the effect of PERK siRNA on *DP5* and *PUMA* expressions (Fig. 5*A* and *B*), suggesting that PERK-ATF3 activation by palmitate leads to *DP5* and *PUMA* expression. In primary β-cells, knockdown of PERK or ATF3 also decreased palmitate induction of *DP5* and *PUMA* (Fig. 5*C*). This is consistent with the presence of a putative ATF3 binding site in the *DP5* promoter region −125 to −85. Exposure of INS-1E cells to palmitate stimulated the association of ATF3 to the *DP5* promoter, showing that this BH3-only protein is a direct target of the PERK-ATF3 pathway (Fig. 5*D*). The *PUMA* promoter, on the other hand, does not contain an ATF3 binding site, suggesting that ATF3 indirectly modulates PUMA.

TRB3-AKT-FoxO3a signaling contributes to the induction of *PUMA* by palmitate. In the microarray analysis, palmitate markedly upregulated *TRB3* (Supplementary Fig. 3 and Supplementary Table 1), an ER stress–inducible and proapoptotic gene in the PERK pathway (33). Because knockdown of CHOP did not change TRB3 expression (Supplementary Fig. 6*G*), we examined the role of ATF3. ATF3 knockdown attenuated TRB3 induction by palmitate (Fig. 5*E*). TRB3 is a pseudokinase that inhibits AKT phosphorylation, leading to the activation of death pathways including GSK-3β. Because AKT inactivates the forkhead box O (FoxO) family of transcription factors, among which FoxO3a has been shown to induce PUMA-dependent apoptosis, we examined whether the TRB3-AKT-FoxO3a pathway plays a role in the induction of *DP5* and *PUMA* by palmitate. The induction of *TRB3* mRNA by palmitate was confirmed at the protein level (Fig. 5*F*), and the FFA decreased both AKT and FoxO3a phosphorylation (Fig. 5*F* and Fig. 6*A*). The dephosphorylation of FoxO3a (Fig. 6*A*)

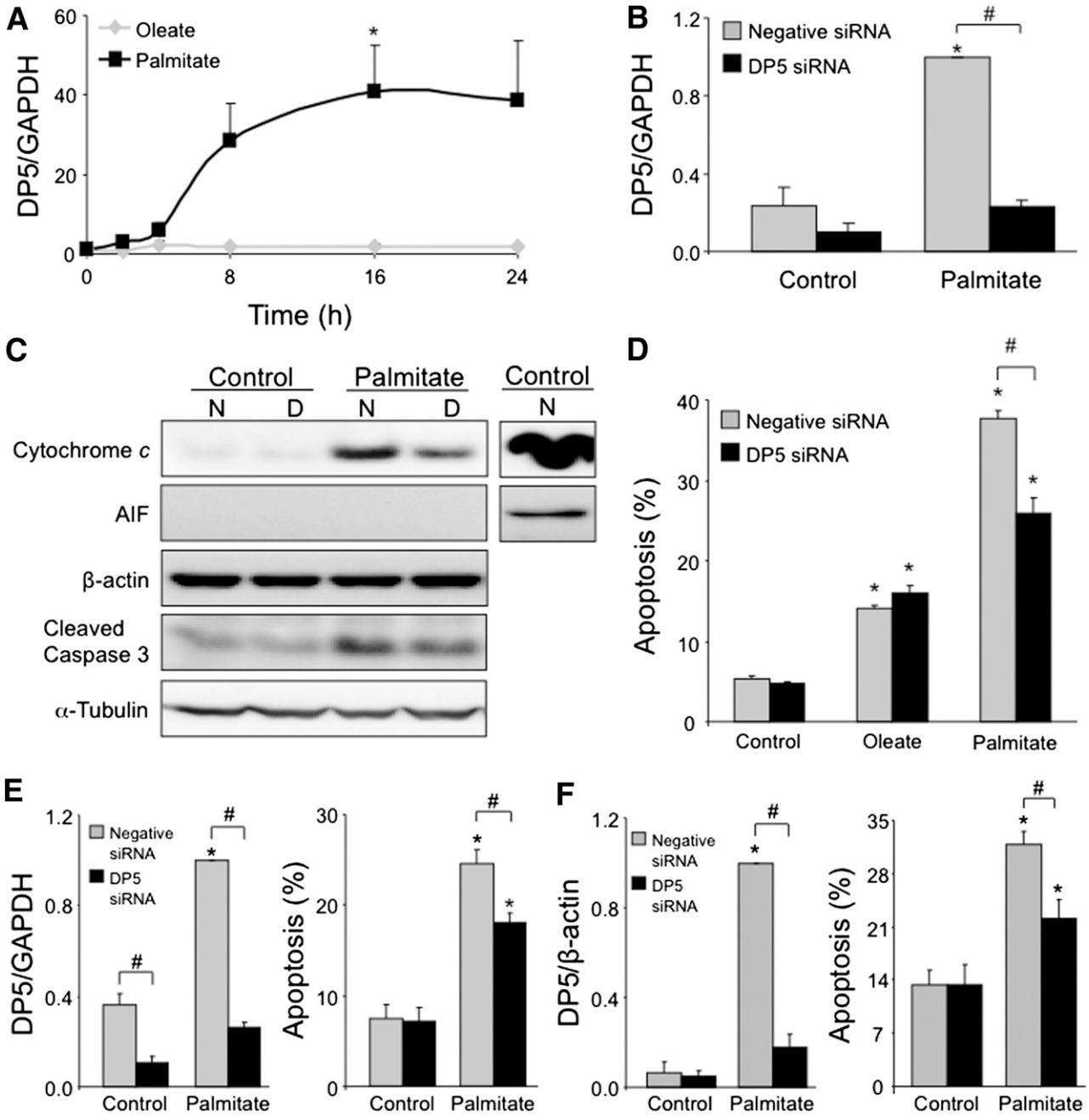

FIG. 2. Palmitate-induced *DP5* expression contributes to β-cell death. *A*: Time-course analysis of *DP5* mRNA expression in oleate- or palmitate-treated INS-1E cells (n = 4). *B*: *DP5* mRNA expression of INS-1E cells transfected with negative or *DP5* siRNA and treated with palmitate for 16 h (n = 5). *C*: Cytoplasmic cytochrome *c* and cleaved caspase 3 levels of INS-1E cells transfected with negative (N) or *DP5* (D) siRNA and palmitate treated for 16 h. Apoptosis-inducing factor (AIF) expression was used as mitochondrial control, β-actin was used as cytoplasmic control, and α-tubulin was used as a control for protein loading for the caspase 3 blot. Separate blots on the right show the noncytosolic fraction, including mitochondria, used as a positive control for cytochrome *c* and AIF blotting. A representative blot of 5 independent experiments is shown. *D*: Apoptosis in INS-1E cells transfected with negative or *DP5* siRNA and then treated with oleate or palmitate for 16 h (n = 3–4). *E*: *DP5* mRNA expression in primary rat β-cells transfected with negative or *DP5* siRNA and treated with palmitate for 24 h, after which apoptosis was assessed (n = 4). *F*: Protection from palmitate-induced cell death by DP5 knockdown in dispersed human islet cells. Cells were transfected with *DP5* siRNA and 2 days later exposed to palmitate for 24 h (n = 4). GAPDH, glyceraldehyde-3-phosphate dehydrogenase. *P < 0.05 against untreated cells. #P < 0.05.

was accompanied by its nuclear translocation (Fig. 6*B* and C), confirming activation of the transcription factor. The knockdown of TRB3 partially prevented early changes in AKT and FoxO3a phosphorylation (Fig. 5*F*). In parallel, TRB3 knockdown decreased palmitate-induced *PUMA* expression (but not *DP5* expression), and reduced lipotoxic β-cell apoptosis (Fig. 5*G* and *H*). Additional TRB3/AKT-independent mechanisms may regulate FoxO3a activation at later time points. In silico analysis of the *DP5* and *PUMA* promoters identified putative FoxO3a binding sites in both BH3-only genes, and ChIP demonstrated that palmitate induces FoxO3a binding to both promoters (Fig. 6*D*). FoxO3a knockdown partially prevented induction of *DP5* and *PUMA* by palmitate (Fig. 6*E*–*F*), showing that the AKT-FoxO3a pathway downstream of ER stress controls the BH3-only gene expression and contributes to β-cell death.

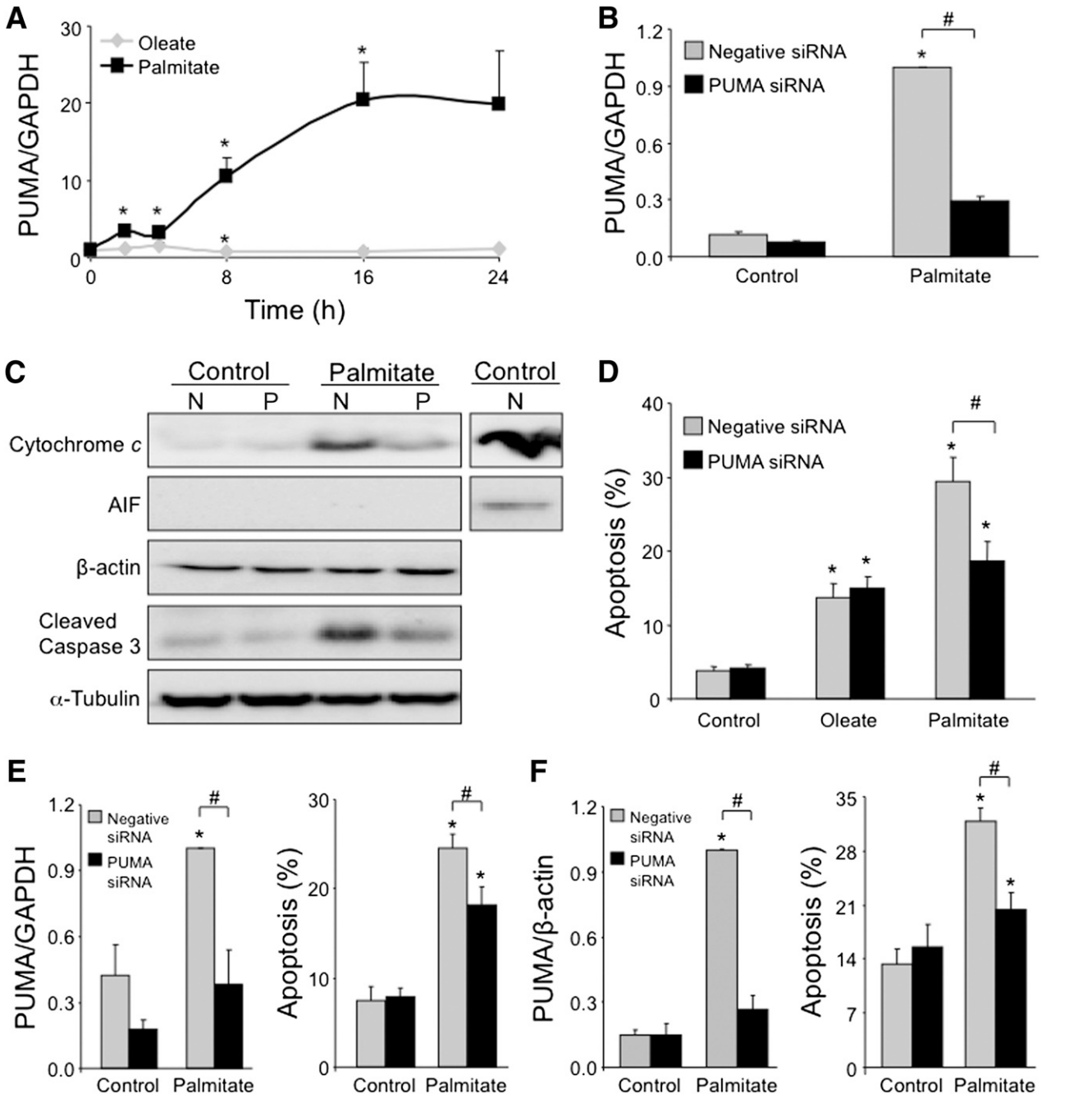

FIG. 3. Palmitate-induced *PUMA* expression contributes to β-cell death. *A*: Time-course analysis of *PUMA* mRNA expression in oleate- and palmitate-treated INS-1E cells (n = 4). *B*: *PUMA* mRNA expression of INS-1E cells transfected with negative or *PUMA* siRNA and treated with palmitate for 16 h (n = 5). *C*: Cytoplasmic cytochrome *c* and cleaved caspase 3 levels in INS-1E cells transfected with negative (N) or *PUMA* (P) siRNA and palmitate treated for 16 h. Apoptosis-inducing factor (AIF) expression was used as mitochondrial control, β-actin was used as cytoplasmic control, and α-tubulin was used as a control for protein loading for the cleaved caspase 3 blot. Separate blots on the right show the noncytosolic fraction, including mitochondria, used as a positive control for cytochrome *c* and AIF blotting. A representative blot of 5 independent experiments is shown. *D*: Apoptosis in INS-1E cells transfected with negative or *PUMA* siRNA and then treated with oleate or palmitate for 16 h (n = 3–4). *E*: *PUMA* mRNA expression in primary rat β-cells transfected with negative or *PUMA* siRNA and treated with palmitate for 24 h, after which apoptosis was assessed (n = 4). *F*: Protection from palmitate-induced cell death by PUMA knockdown in dispersed human islet cells. Cells were transfected with *PUMA* siRNA and 2 days later exposed to palmitate for 24 h (n = 4). GAPDH, glyceraldehyde-3-phosphate dehydrogenase. *$P < 0.05$ against untreated cells. #$P < 0.05$.

***DP5*$^{-/-}$ mice are protected from HFD-induced loss of glucose tolerance and have increased β-cell mass.** Because DP5 is upstream of PUMA (17) and DP5 but not PUMA knockdown provides complete β-cell protection from palmitate at early time points (data not shown), we selected *DP5*$^{-/-}$ mice for in vivo studies. *DP5*$^{-/-}$ and WT mice were given standard chow or HFD (fat 60% of caloric intake). After 12 weeks, the two HFD-fed genotypes had similar weight gain and insulin sensitivity (Fig. 7*A* and *B*). In line with this, similar weight gain, perirenal fat accumulation and hepatic insulin-induced AKT phosphorylation were observed in WT or *DP5* knockout mice after 25 weeks of chow or HFD (data not shown). *DP5* mRNA expression increased threefold in islets from HFD-fed WT mice

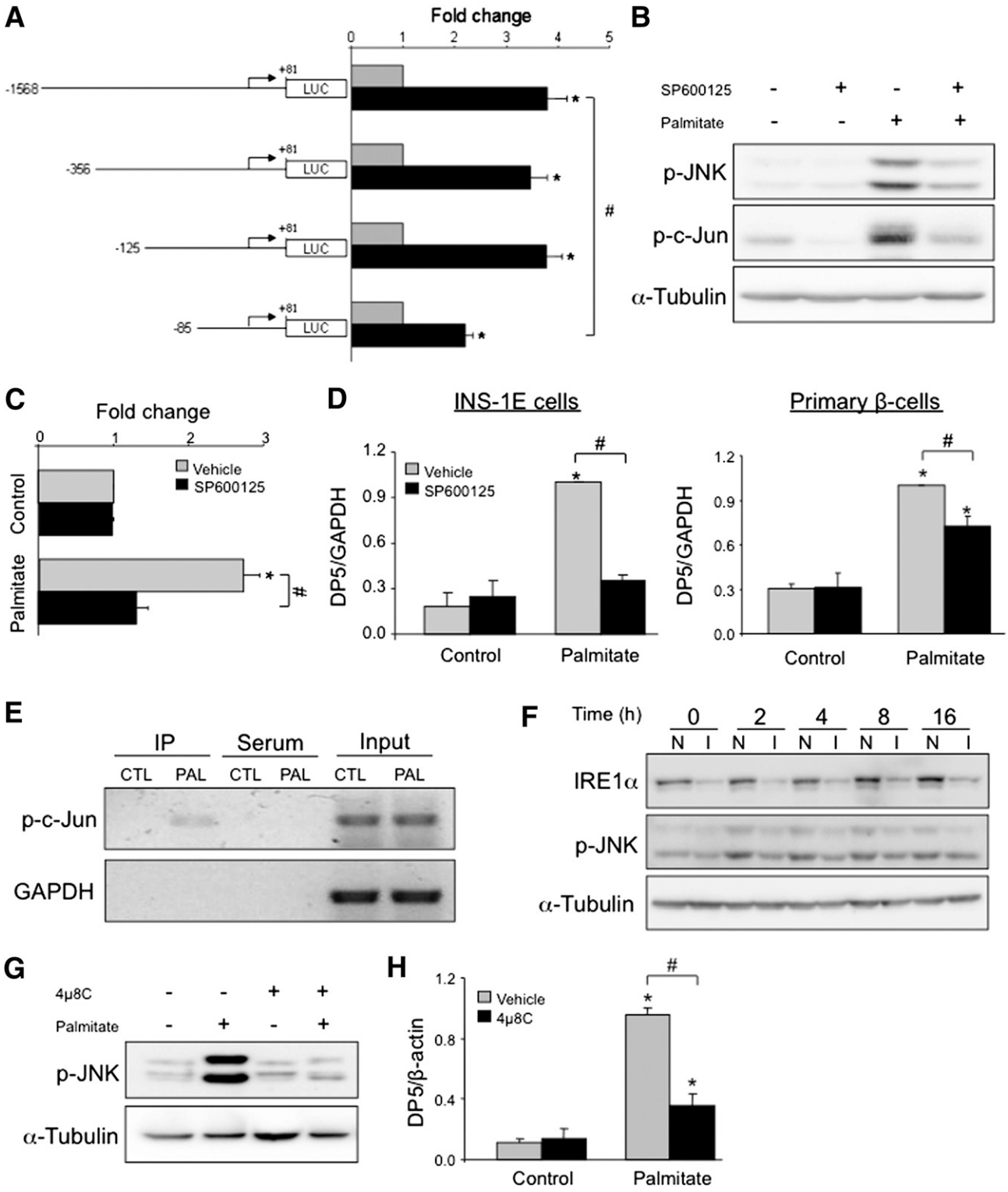

FIG. 4. JNK activation contributes to *DP5* induction by palmitate in β-cells. *A*: *DP5* promoter study of INS-1E cells transfected with *DP5* promoter fragments of different lengths (*left*) and the control plasmid CMV-RL and then treated with palmitate for 16 h. Firefly luciferase (LUC) activity was normalized to Renilla luciferase activity and expressed as fold induction of control ($n = 4$). *B*: JNK and c-Jun phosphorylation in INS-1E cells treated with palmitate or the JNK inhibitor SP600125 (10 μmol/L) for 16 h. A representative blot of 3 independent experiments is shown. *C*: *DP5* promoter study of INS-1E cells transfected with the full *DP5* promoter and treated with the JNK inhibitor SP600125 as in *B* ($n = 4$). *D*: *DP5* mRNA expression of INS-1E cells (*left*) or primary β-cells (*right*) exposed to palmitate for 16 h or 24 h, respectively, in the presence or absence of SP600125 ($n = 4$). *E*: ChIP showing the binding of *p*-c-Jun to the *DP5* promoter in INS-1E cells treated with palmitate (PAL) or left untreated (CTL) for 4 h ($n = 3$). Samples were incubated with *p*-c-Jun antibody (IP) or goat serum (serum, negative control). Input is total DNA from the samples. A representative image of 3 independent experiments is shown. The glyceraldehyde-3-phosphate dehydrogenase (GAPDH) promoter was used as a negative control. *F*: INS-1E cells were transfected with negative (N) or IRE1α (I) siRNA and after 3 days treated with palmitate for the indicated times. A representative blot for IRE1α protein expression and JNK protein phosphorylation is shown (n = 4). *G* and *H*: JNK phosphorylation (*G*) and *DP5* mRNA expression (*H*) ($n = 3$–4) in INS-1E cells treated with palmitate and/or the IRE1 inhibitor 4μ8C (25 μmol/L) for 16 h. In *G*, a representative image of 4 independent experiments is shown. *$P < 0.05$ against untreated cells. #$P < 0.05$.

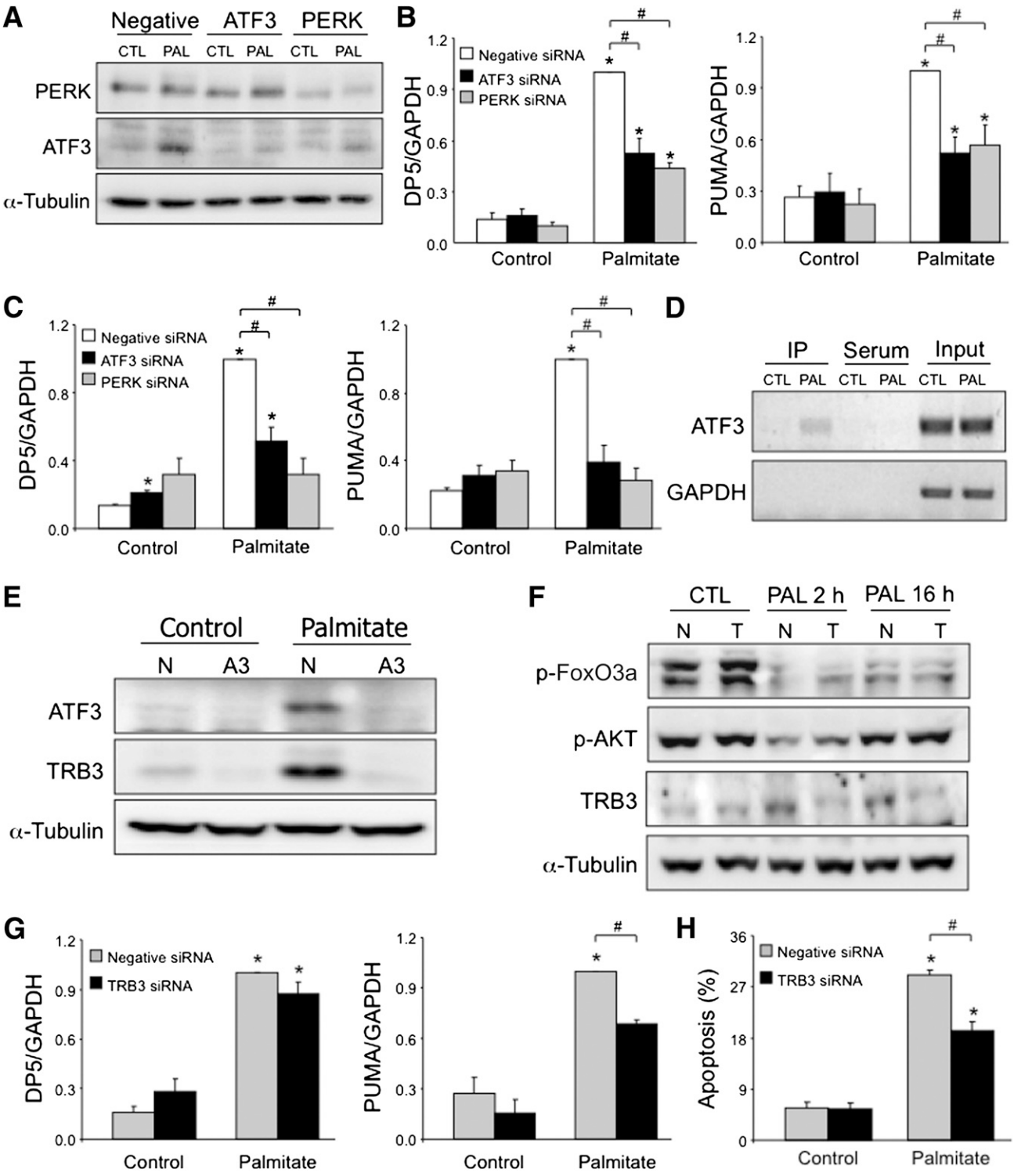

FIG. 5. The PERK-ATF3 pathway modulates *DP5* and *PUMA* expressions. *A*: PERK and ATF3 protein expressions of INS-1E cells transfected with negative, ATF3, or PERK siRNA and treated 3 days after with palmitate (PAL) or left untreated (CTL) for 16 h. A representative blot of 3 independent experiments is shown. B: *DP5* and *PUMA* mRNA expressions of INS-1E cells transfected and treated as in *A* (n = 4). *C*: *DP5* and *PUMA* mRNA expressions of primary rat β-cells transfected with negative, ATF3, or PERK siRNA and 3 days after treated with palmitate for 24 h. *D*: ChIP showing the binding of ATF3 to the *DP5* promoter in INS-1E cells treated with palmitate (PAL) or left untreated (CTL) for 8 h (n = 3). Samples were incubated with ATF3 antibody (IP) or goat serum (serum, negative control). Input is total DNA from the samples. The glyceraldehyde-3-phosphate dehydrogenase (GAPDH) promoter was used as a negative control. A representative image of 3 independent experiments is shown. *E*: ATF3 and TRB3 protein expression of INS-1E cells transfected with negative (N) or ATF3 (A3) siRNA and treated with palmitate for 16 h. A representative blot of 3 independent experiments is shown. *F*: FoxO3a and AKT protein phosphorylation and TRB3 protein expression in INS-1E cells transfected with negative (N) or TRB3 (T) siRNA and treated with palmitate (PAL) or left untreated (CTL) for the indicated times. A representative blot of 4 independent experiments is shown. *G*: *DP5* and *PUMA* mRNA expressions in INS-1E cells transfected with negative or TRB3 siRNA and treated with palmitate for 16 h (n = 4). *H*: Apoptosis in INS-1E cells transfected and treated as in *G* (n = 4). *$P < 0.05$ against untreated cells. #$P < 0.05$.

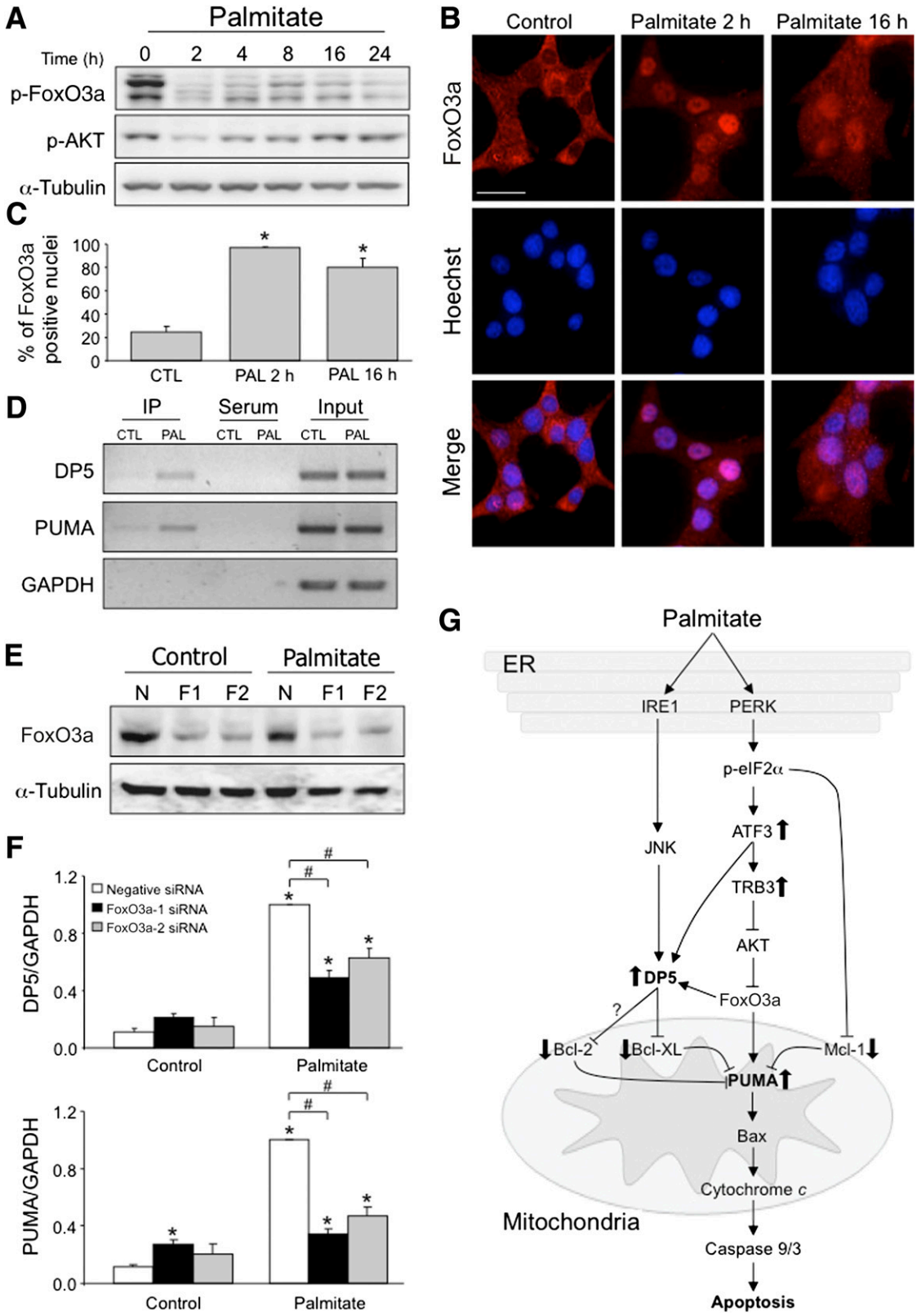

FIG. 6. Palmitate-induced FoxO3a activation modulates *DP5* and *PUMA* expressions. *A*: Time-course analysis of FoxO3a and AKT phosphorylation of INS-1E cells exposed to palmitate. A representative blot of 5 independent experiments is shown. *B* and *C*: Representative immunofluorescence picture (*B*, bar represents 20 μm) and quantification (*C*) of FoxO3a-positive nuclei in INS-1E cells treated with palmitate (PAL) for the indicated times. In *B*, FoxO3a is stained red and DNA is stained blue ($n = 3$). *D*: ChIP showing increased binding of FoxO3a to the *DP5* and *PUMA* promoters in INS-1E cells treated for 4 h with palmitate (PAL) as compared with untreated cells (CTL). Samples were incubated with FoxO3a antibody (IP) or goat serum (serum, negative control). Input is total DNA from the samples. The glyceraldehyde-3-phosphate dehydrogenase (GAPDH) promoter was used as a negative control. A representative image of 3 independent experiments is shown. *E*: FoxO3a protein expression in INS-1E cells transfected with negative or two different siRNAs targeting FoxO3a (F1 and F2) and then treated with palmitate for 16 h ($n = 3$–4). *F*: *DP5* and *PUMA* mRNA expressions in INS-1E cells transfected and treated as in *E*. *G*: Schematic representation of the main findings; for details see text. Thick arrow up indicates induction by palmitate treatment and thick arrow down indicates downregulation. *$P < 0.05$ against untreated cells. #$P < 0.05$. (A high-quality digital representation of this figure is available in the online issue.)

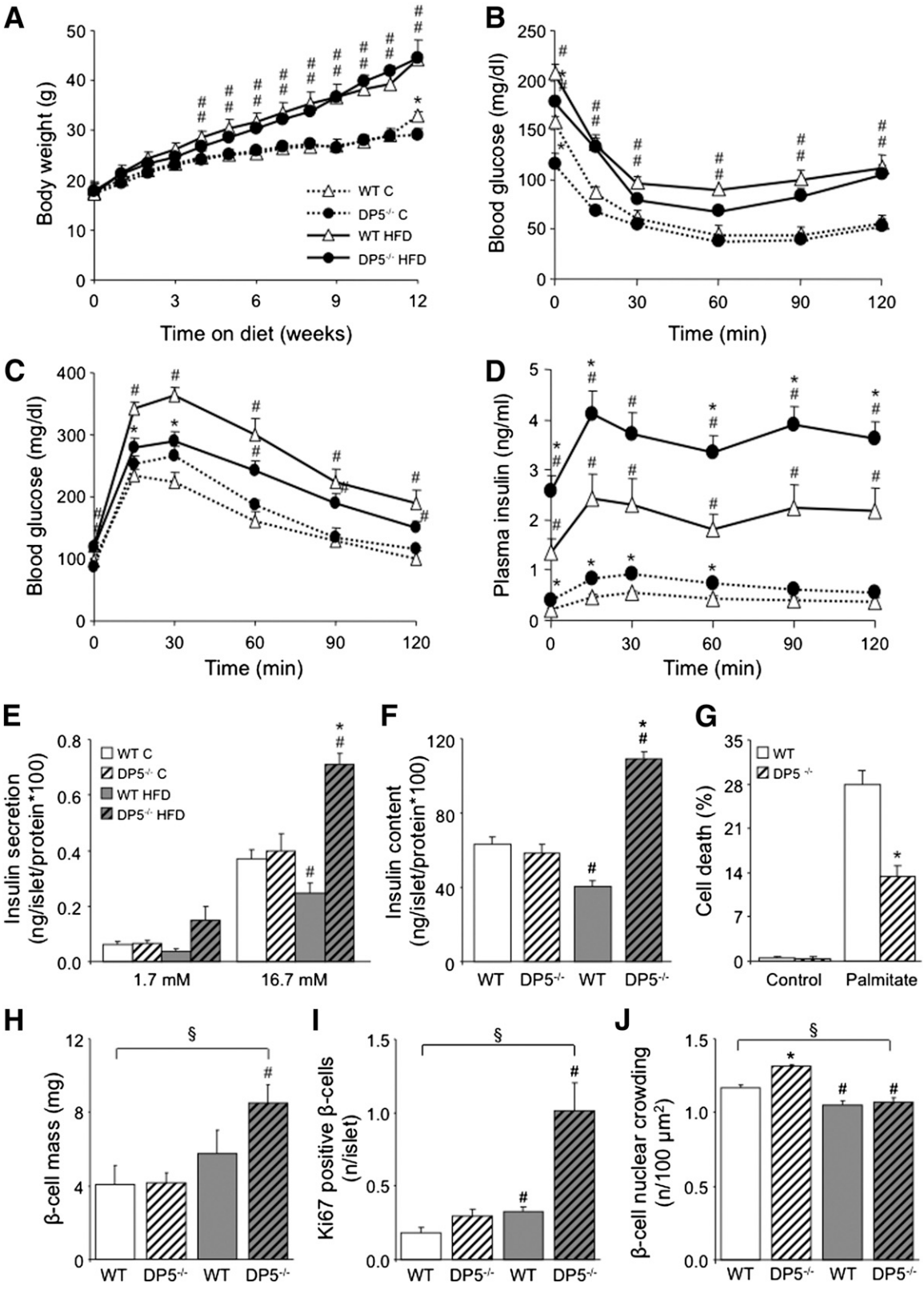

FIG. 7. ***DP5*** **knockout mice are partially protected from HFD-induced impaired glucose tolerance.** ***A*****: Weight gains of WT or** $DP5^{-/-}$ **mice receiving standard chow (C,** ***dotted line*****) and HFD (*full line*) were similar.** ***B*****: Blood glucose levels during intraperitoneal insulin tolerance test (*n* = 8–15).** ***C*** **and** ***D*****: Blood glucose (*C*) and plasma insulin (*D*) levels during intraperitoneal glucose tolerance test (*n* = 8–15).** ***E*** **and** ***F*****: Glucose-stimulated insulin secretion (*E*) and insulin content (*F*) in isolated islets, normalized by total protein content. Insulin secretion at 16.7 mmol/L glucose was significantly higher than that at 1.7 mmol/L for all conditions ($P < 0.01$; *n* = 4).** ***G*****: Cell death in WT and** $DP5^{-/-}$ **mouse islets treated for 2 days with 0.5 mmol/L palmitate (*n* = 3).** ***H*****: Pancreatic β-cell mass was assessed in WT and** $DP5^{-/-}$ **mice maintained on chow or HFD for a total period of 25 weeks (*n* = 5–6).** ***I*****: The number of Ki67-positive (dividing) β-cells per islet increased in the HFD-fed mice (*n* = 3–4).** ***J*****: β-Cell nuclear crowding was measured to evaluate β-cell hypertrophy (*n* = 3–4).** $*P < 0.05$ **for the comparison between genotypes on the same diet.** $\#P < 0.05$ **for the comparison between chow and HFD.** $\S P < 0.05$ **as indicated.**

compared with chow-fed WT mice ($P = 0.17$, $n = 5–6$). *DP5*$^{-/-}$ mice were protected from HFD-induced diabetes (Fig. 7*C*) as a result of strikingly increased insulin secretion (Fig. 7*D*). Islets isolated from HFD-fed *DP5*$^{-/-}$ mice contained and secreted twofold more insulin after glucose stimulation (Fig. 7*E-F*), suggesting a protective effect at the β-cell level. The lack of the *DP5* gene also protected mouse islets in vitro from palmitate-induced cell death (Fig. 7*G*). This resistance to lipotoxicity was paralleled by a doubling of β-cell mass in HFD-fed *DP5*$^{-/-}$ mice but not in WT mice (Fig. 7*H*), confirming the physiological role of DP5 in vivo. We could not detect apoptotic β-cells in vivo in HFD-fed WT mice (data not shown) and were therefore unable to assess the putative protective role of DP5 deficiency. Increased β-cell proliferation, assessed by Ki67 staining (Fig. 7*I*), and β-cell hypertrophy (Fig. 7*J*) likely contribute to the greater β-cell mass of *DP5*$^{-/-}$ mice. Thus DP5 may not only play a role in β-cell apoptosis but also serve as a brake on β-cell growth and proliferation.

DISCUSSION

Failure of the pancreatic β-cells to compensate for high insulin needs is central to the pathogenesis of T2D, and several studies have reported a significant decrease in β-cell mass in T2D (2,26). Chronic exposure to FFAs causes loss of functional β-cell mass (34,35) and may contribute to T2D. Saturated lipids are harmful to β-cells, and pronounced ER stress signaling (especially in the PERK pathway) has been proposed to mediate lipotoxic apoptosis (7–10,15). Execution of FFA-induced apoptosis occurs through the mitochondrial pathway, as indicated by cytochrome *c* release from the mitochondria after palmitate treatment (13,36,37), but it remained to be clarified how palmitate-induced ER stress crosstalks with the mitochondria to culminate in β-cell death. We have now answered this question, showing that palmitate transcriptionally induces the BH3-only proteins DP5 and PUMA through PERK-dependent *ATF3* expression (Fig. 6*G*).

In the hierarchical model for Bax/Bak activation, the BH3-only "sensitizer" proteins DP5, Bad, Bik, Bnip3, Bmf, and Noxa neutralize the prosurvival Bcl-2 proteins, allowing the BH3-only "activators" PUMA, Bim, and tBid to be released to activate Bax/Bak (38,39). The use of the different pro- and antiapoptotic proteins after a proapoptotic stimulus is cell and context dependent.

Palmitate decreases Bcl-2 expression (13); however its contribution to lipotoxic β-cell death had not been examined. We now show that the decreased Bcl-2 protein expression in palmitate-exposed β-cells occurs in conjunction with mitochondrial fragmentation and apoptosis. A reduction in Bcl-XL protein was seen only after 24 h of palmitate exposure, suggesting that decreased Bcl-XL levels are not pivotal in palmitate-induced apoptosis. A role for Mcl-1 protein downregulation has also been reported in palmitate- and ER stress–induced β-cell apoptosis (40).

The BH3-only prodeath sensitizers and activators in lipotoxicity are essentially unknown. Gene expression profiling of palmitate-treated β-cells indicated that palmitate induced a gene expression signature of ER stress at the early time-point (6 h). At a later time-point (14 h), palmitate upregulated apoptosis-related genes, shifting from an adaptive response to one geared for cell death. As part of the proapoptotic signal network, there was upregulation of *DP5* and *PUMA*, genes for two BH3-only proteins previously shown to play a role in apoptosis of β-cells exposed to cytokines (31,41). Knockdown of the BH3-only sensitizer DP5 and the activator PUMA protected β-cells from palmitate, establishing their contribution to saturated FFA-induced apoptosis. Because the protection is partial in rat β-cells, other BH3-only proteins or alternative death mechanisms may play additional roles. Of note, oleate did not increase *DP5* or *PUMA* expression, in keeping with the observation that this FFA is much less toxic (5,9).

We next set out to identify the mechanism of induction of these prodeath proteins by palmitate. Although the upstream UPR has been characterized in detail, the downstream transduction mechanisms through which ER stress connects to mitochondrial apoptosis have remained elusive. By promoter analysis, we identified a putative c-Jun binding site in the *DP5* promoter, and confirmed *p*-c-Jun binding by ChIP. Inhibition of IRE1-dependent JNK activation reduced *DP5* promoter activation and mRNA induction by palmitate. These results are consistent with our previous finding that JNK inhibition protects against lipotoxic β-cell death (9). JNK regulates the intrinsic death pathway through transcriptional as well as posttranscriptional modifications of Bcl-2 family members (42,43).

The BH3-only activator *PUMA* was not induced by JNK, p53, or NF-κB, previously shown to modulate *PUMA* expression (29–31,44). We therefore examined the role of ER stress in *PUMA* expression. Of the three branches of the UPR, sustained activation of the PERK pathway plays a large part in β-cell apoptosis (14,15). Downstream of PERK, CHOP contributes to palmitate-induced apoptosis (9). *CHOP* deletion also improves glycemic control and prevents β-cell loss in mouse models of T2D (45). ATF3 is also induced by PERK; its role in β-cell death is more controversial. ATF3 knockout confers minor protection against cytokine-induced islet cell apoptosis (46) which may involve the regulation of the insulin receptor substrate 2 (47). In HFD-fed mice, on the other hand, ATF3 is protective by regulating insulin synthesis (48). We have now demonstrated that PERK-induced ATF3, but not ATF4-CHOP, induces both *PUMA* and *DP5*. Interestingly, the mechanisms by which ATF3 regulates *DP5* and *PUMA* expressions are not similar. ATF3 directly modulates *DP5* mRNA expression, as suggested by its binding to the *DP5* promoter, whereas *PUMA* regulation depends on a complex pathway involving TRB3, AKT, and FoxO3a (Fig. 6*G*).

TRB3 was identified as a proapoptotic effector of CHOP and ATF4 (49). Increased *TRB3* expression was observed in islets from T2D donors and HFD-fed mice (50). In the same study, interaction between TRB3 and ATF4 decreased insulin secretion by reducing the expression of exocytosis-related genes. We show here that *TRB3* is induced by ATF3 but not CHOP and causes FoxO3a-dependent *PUMA* induction and cell death. In other cell types, FoxO3a has been shown to induce *PUMA* expression independently of p53 (51). We also demonstrated that *DP5* upregulation is partially FoxO3a dependent, which is consistent with the presence of a putative FoxO3a binding site in its promoter. This *DP5* induction by FoxO3a is apparently TRB3-independent, suggesting alternative FoxO3a activation mechanism.

The physiological relevance of these findings was examined in *DP5*$^{-/-}$ mice exposed to HFD. Compared with WT mice, the *DP5*$^{-/-}$ mice were resistant to lipotoxic loss of glucose tolerance as a result of significantly greater glucose-stimulated insulin secretion and an adaptive increase in β-cell mass. Interestingly, β-cell proliferation and hypertrophy were increased in HFD-fed *DP5*$^{-/-}$ mice,

pointing to a hitherto unknown inhibitory role of *DP5* in cell growth and the cell cycle. Because the mice were whole-body knockouts, it cannot be excluded that *DP5* deficiency also exerts beneficial effects in peripheral tissues.

In conclusion, lipotoxic ER stress causes JNK- and PERK-dependent ATF3 and TRB3-FOXO3a activation, and these transcription factors regulate expression of Bcl-2 family members. Palmitate engages the mitochondrial pathway of cell death through induction of the BH3-only sensitizer DP5, loss of antiapoptotic Bcl-2 and Mcl-1, and upregulation of the BH3-only activator PUMA, culminating in the activation of Bax/Bak and mitochondrial permeabilization (Fig. 6*G*). These results provide insight into the mechanisms of lipotoxic β-cell ER stress and identify hitherto unknown transcriptional regulation and signal transduction between ER stress and mitochondrial apoptosis. The findings also delineate potential new areas for β-cell therapy in the prevention and treatment of T2D.

ACKNOWLEDGMENTS

This work was supported by the European Union (Collaborative Projects CEED3 and BetaBat in the Framework Program 7), a European Foundation for the Study of Diabetes (EFSD)/Lilly grant, the Fonds National de la Recherche Scientifique (FNRS), Fonds de la Recherche Scientifique Médicale (FRSM) and Actions de Recherche Concertées de la Communauté Française (ARC), Belgium. D.A.C. was supported by an FNRS post-doctoral fellowship, E.N.G. was supported by an EMBO long-term fellowship, and J.-M.V. is research director at the FNRS.

No potential conflicts of interest relevant to this article were reported.

D.A.C., E.N.G., D.L.E, and M.C. contributed to the experimental design of the study. D.A.C., M.I.-E., E.N.G., C.M.G., N.N., I.M., M.F., J.-M.V., C.G., and D.R. carried out experiments, helped with data analysis, or both. C.M., L.M., P.M., H.P.H., and D.R. contributed materials and data interpretation. D.A.C., M.I.-E., E.N.G., D.L.E, and M.C. analyzed and interpreted the data. D.A.C., D.L.E, and M.C. wrote the manuscript. M.C. is the guarantor of this work and, as such, had full access to all the data in the study and takes responsibility for the integrity of the data and the accuracy of the data analysis.

The authors thank Mingtao Li, Sun Yat-sen University, for providing the *DP5* promoter; Lin Zhang, University of Pittsburgh, for the *PUMA* promoter; Andrea Jurisicova, University of Toronto, and Gabriel Nuñez, University of Michigan, for the *DP5*$^{-/-}$ mice; Miriam Hernangomez Herrero, Université Libre de Bruxelles, for help with the mouse experiments; and Gilbert Vandenbroeck, Marie-Anne Neef, Maryse Urbain, Anyishai Musuaya, Stephanie Mertens, and Rachid Makhnas, all from Université Libre de Bruxelles, for expert technical assistance.

REFERENCES

1. International Diabetes Federation. *IDF Diabetes Atlas*. 4th ed. Brussels, International Diabetes Federation Executive Office, 2009
2. Butler AE, Janson J, Bonner-Weir S, Ritzel R, Rizza RA, Butler PC. β-cell deficit and increased β-cell apoptosis in humans with type 2 diabetes. Diabetes 2003;52:102–110
3. Swinburn BA, Boyce VL, Bergman RN, Howard BV, Bogardus C. Deterioration in carbohydrate metabolism and lipoprotein changes induced by modern, high fat diet in Pima Indians and Caucasians. J Clin Endocrinol Metab 1991;73:156–165
4. Kaiyala KJ, Prigeon RL, Kahn SE, Woods SC, Porte D Jr, Schwartz MW. Reduced β-cell function contributes to impaired glucose tolerance in dogs made obese by high-fat feeding. Am J Physiol 1999;277:E659–E667
5. Cnop M, Hannaert JC, Hoorens A, Eizirik DL, Pipeleers DG. Inverse relationship between cytotoxicity of free fatty acids in pancreatic islet cells and cellular triglyceride accumulation. Diabetes 2001;50:1771–1777
6. Zhou YP, Grill VE. Long-term exposure of rat pancreatic islets to fatty acids inhibits glucose-induced insulin secretion and biosynthesis through a glucose fatty acid cycle. J Clin Invest 1994;93:870–876
7. Kharroubi I, Ladrière L, Cardozo AK, Dogusan Z, Cnop M, Eizirik DL. Free fatty acids and cytokines induce pancreatic β-cell apoptosis by different mechanisms: role of nuclear factor-κB and endoplasmic reticulum stress. Endocrinology 2004;145:5087–5096
8. Karaskov E, Scott C, Zhang L, Teodoro T, Ravazzola M, Volchuk A. Chronic palmitate but not oleate exposure induces endoplasmic reticulum stress, which may contribute to INS-1 pancreatic β-cell apoptosis. Endocrinology 2006;147:3398–3407
9. Cunha DA, Hekerman P, Ladrière L, et al. Initiation and execution of lipotoxic ER stress in pancreatic β-cells. J Cell Sci 2008;121:2308–2318
10. Laybutt DR, Preston AM, Akerfeldt MC, et al. Endoplasmic reticulum stress contributes to beta cell apoptosis in type 2 diabetes. Diabetologia 2007;50:752–763
11. Eizirik DL, Cardozo AK, Cnop M. The role for endoplasmic reticulum stress in diabetes mellitus. Endocr Rev 2008;29:42–61
12. Ron D, Walter P. Signal integration in the endoplasmic reticulum unfolded protein response. Nat Rev Mol Cell Biol 2007;8:519–529
13. Cunha DA, Ladrière L, Ortis F, et al. Glucagon-like peptide-1 agonists protect pancreatic β-cells from lipotoxic endoplasmic reticulum stress through upregulation of BiP and JunB. Diabetes 2009;58:2851–2862
14. Ladrière L, Igoillo-Esteve M, Cunha DA, et al. Enhanced signaling downstream of ribonucleic acid-activated protein kinase-like endoplasmic reticulum kinase potentiates lipotoxic endoplasmic reticulum stress in human islets. J Clin Endocrinol Metab 2010;95:1442–1449
15. Cnop M, Ladriere L, Hekerman P, et al. Selective inhibition of eukaryotic translation initiation factor 2 α dephosphorylation potentiates fatty acid-induced endoplasmic reticulum stress and causes pancreatic β-cell dysfunction and apoptosis. J Biol Chem 2007;282:3989–3997
16. Youle RJ, Strasser A. The BCL-2 protein family: opposing activities that mediate cell death. Nat Rev Mol Cell Biol 2008;9:47–59
17. Kim H, Rafiuddin-Shah M, Tu HC, et al. Hierarchical regulation of mitochondrion-dependent apoptosis by BCL-2 subfamilies. Nat Cell Biol 2006;8:1348–1358
18. Tournier C, Hess P, Yang DD, et al. Requirement of JNK for stress-induced activation of the cytochrome c-mediated death pathway. Science 2000;288:870–874
19. Kim BJ, Ryu SW, Song BJ. JNK- and p38 kinase-mediated phosphorylation of Bax leads to its activation and mitochondrial translocation and to apoptosis of human hepatoma HepG2 cells. J Biol Chem 2006;281:21256–21265
20. Lei K, Davis RJ. JNK phosphorylation of Bim-related members of the Bcl2 family induces Bax-dependent apoptosis. Proc Natl Acad Sci USA 2003;100:2432–2437
21. Donovan N, Becker EB, Konishi Y, Bonni A. JNK phosphorylation and activation of BAD couples the stress-activated signaling pathway to the cell death machinery. J Biol Chem 2002;277:40944–40949
22. Akazawa Y, Cazanave S, Mott JL, et al. Palmitoleate attenuates palmitate-induced Bim and PUMA up-regulation and hepatocyte lipoapoptosis. J Hepatol 2010;52:586–593
23. Ma C, Ying C, Yuan Z, et al. dp5/HRK is a c-Jun target gene and required for apoptosis induced by potassium deprivation in cerebellar granule neurons. J Biol Chem 2007;282:30901–30909
24. Santin I, Moore F, Colli ML, et al. PTPN2, a candidate gene for type 1 diabetes, modulates pancreatic β-cell apoptosis via regulation of the BH3-only protein Bim. Diabetes 2011;60:3279–3288
25. Cross BC, Bond PJ, Sadowski PG, et al. The molecular basis for selective inhibition of unconventional mRNA splicing by an IRE1-binding small molecule. Proc Natl Acad Sci USA 2012;109:E869–E878
26. Rahier J, Guiot Y, Goebbels RM, Sempoux C, Henquin JC. Pancreatic β-cell mass in European subjects with type 2 diabetes. Diabetes Obes Metab 2008;10(Suppl. 4):32–42
27. Sempoux C, Guiot Y, Lefevre A, et al. Neonatal hyperinsulinemic hypoglycemia: heterogeneity of the syndrome and keys for differential diagnosis. J Clin Endocrinol Metab 1998;83:1455–1461
28. Ortis F, Naamane N, Flamez D, et al. Cytokines interleukin-1β and tumor necrosis factor-α regulate different transcriptional and alternative splicing networks in primary β-cells. Diabetes 2010;59:358–374
29. Nakano K, Vousden KH. PUMA, a novel proapoptotic gene, is induced by p53. Mol Cell 2001;7:683–694

30. Wang P, Qiu W, Dudgeon C, et al. PUMA is directly activated by NF-κB and contributes to TNF-α-induced apoptosis. Cell Death Differ 2009;16:1192–1202
31. Gurzov EN, Germano CM, Cunha DA, et al. p53 up-regulated modulator of apoptosis (PUMA) activation contributes to pancreatic β-cell apoptosis induced by proinflammatory cytokines and endoplasmic reticulum stress. J Biol Chem 2010;285:19910–19920
32. McCullough KD, Martindale JL, Klotz LO, Aw TY, Holbrook NJ. Gadd153 sensitizes cells to endoplasmic reticulum stress by down-regulating Bcl2 and perturbing the cellular redox state. Mol Cell Biol 2001;21:1249–1259
33. Qian B, Wang H, Men X, et al. TRIB3 is implicated in glucotoxicity- and endoplasmic reticulum stress-induced β-cell apoptosis [published correction appears in J Endocrinol 2009;200:243 and 2009;203:399]. J Endocrinol 2008;199:407–416
34. Cnop M, Igoillo-Esteve M, Cunha DA, Ladrière L, Eizirik DL. An update on lipotoxic endoplasmic reticulum stress in pancreatic β-cells. Biochem Soc Trans 2008;36:909–915
35. Poitout V. Glucolipotoxicity of the pancreatic beta-cell: myth or reality? Biochem Soc Trans 2008;36:901–904
36. Maedler K, Spinas GA, Dyntar D, Moritz W, Kaiser N, Donath MY. Distinct effects of saturated and monounsaturated fatty acids on β-cell turnover and function. Diabetes 2001;50:69–76
37. Maestre I, Jordán J, Calvo S, et al. Mitochondrial dysfunction is involved in apoptosis induced by serum withdrawal and fatty acids in the β-cell line INS-1. Endocrinology 2003;144:335–345
38. Kuwana T, Bouchier-Hayes L, Chipuk JE, et al. BH3 domains of BH3-only proteins differentially regulate Bax-mediated mitochondrial membrane permeabilization both directly and indirectly. Mol Cell 2005;17:525–535
39. Ren D, Tu HC, Kim H, et al. BID, BIM, and PUMA are essential for activation of the BAX- and BAK-dependent cell death program. Science 2010;330:1390–1393
40. Allagnat F, Cunha D, Moore F, Vanderwinden JM, Eizirik DL, Cardozo AK. Mcl-1 downregulation by pro-inflammatory cytokines and palmitate is an early event contributing to β-cell apoptosis. Cell Death Differ 2011;18:328–337
41. Gurzov EN, Ortis F, Cunha DA, et al. Signaling by IL-1β+IFN-γ and ER stress converge on DP5/Hrk activation: a novel mechanism for pancreatic β-cell apoptosis. Cell Death Differ 2009;16:1539–1550
42. Pierucci D, Cicconi S, Bonini P, et al. NGF-withdrawal induces apoptosis in pancreatic beta cells in vitro. Diabetologia 2001;44:1281–1295
43. Harris CA, Johnson EM Jr. BH3-only Bcl-2 family members are coordinately regulated by the JNK pathway and require Bax to induce apoptosis in neurons. J Biol Chem 2001;276:37754–37760
44. Cazanave SC, Mott JL, Elmi NA, et al. JNK1-dependent PUMA expression contributes to hepatocyte lipoapoptosis. J Biol Chem 2009;284:26591–26602
45. Song B, Scheuner D, Ron D, Pennathur S, Kaufman RJ. Chop deletion reduces oxidative stress, improves β cell function, and promotes cell survival in multiple mouse models of diabetes. J Clin Invest 2008;118:3378–3389
46. Hartman MG, Lu D, Kim ML, et al. Role for activating transcription factor 3 in stress-induced β-cell apoptosis. Mol Cell Biol 2004;24:5721–5732
47. Li D, Yin X, Zmuda EJ, et al. The repression of IRS2 gene by ATF3, a stress-inducible gene, contributes to pancreatic β-cell apoptosis. Diabetes 2008;57:635–644
48. Zmuda EJ, Qi L, Zhu MX, Mirmira RG, Montminy MR, Hai T. The roles of ATF3, an adaptive-response gene, in high-fat-diet-induced diabetes and pancreatic β-cell dysfunction. Mol Endocrinol 2010;24:1423–1433
49. Ohoka N, Yoshii S, Hattori T, Onozaki K, Hayashi H. TRB3, a novel ER stress-inducible gene, is induced via ATF4-CHOP pathway and is involved in cell death. EMBO J 2005;24:1243–1255
50. Liew CW, Bochenski J, Kawamori D, et al. The pseudokinase tribbles homolog 3 interacts with ATF4 to negatively regulate insulin exocytosis in human and mouse β cells. J Clin Invest 2010;120:2876–2888
51. You H, Pellegrini M, Tsuchihara K, et al. FOXO3a-dependent regulation of Puma in response to cytokine/growth factor withdrawal. J Exp Med 2006;203:1657–1663